JOURNAL OF OPTOELECTRONICS AND ADVANCED MATERIALS Vol. 8, No. 1, February 2006, p. 7 – 12

Epitaxial-quality PZT: insulator or semiconductor?

L. PINTILIE[a*], M. LISCA[a,b], M. ALEXE[a]
[a]Max Planck Institute for Microstructure Physics, Weinberg 2, 06120, Halle, Germany
[b]National Institute of Materials Physics, Bucharest-Magurele, P.O. Box MG-7, 077125, Romania

The lead zirconate-titanate (PZT) epitaxial thin films are analyzed as being p-type, wide-gap semiconductors with standard Schottky contacts. The results of the hysteresis, capacitance-voltage (C-V), and current-voltage (I-V) measurements are explained in the frame of the classical model for metal-semiconductor Schottky contacts, in which the effect of the ferroelectric polarization on band-bending was considered. The presence of the deep traps was also considered and their effect on the measured quantities was discussed. The free carrier concentration was estimated to about 3×10^{18} cm^{-3}, with a remnant polarization of 40 μC/cm^2, and with an effective density of the fixed charges in the depletion region of about 1.8×10^{19} cm^{-3}.

(Received October 14, 2005; accepted January 26, 2006)

Keywords: PZT, Semiconductor, Insulator, Deep traps, Polarization

1. Introduction

The ferroelectric perovskites (ABO_3) are traditionally considered insulating materials mostly due to the ionic nature of the chemical bonds [1]. Recently, it was shown that the origin of ferroelectricity in the most representative perovskites, barium titanate (BTO) and lead titanate (PTO), is quite different and is directly related with the nature of the chemical bonds [2]. The electronic properties are also dependent on the nature of the chemical bonds. In BTO the Ba-O bond is purely ionic, while in PTO the Pb-O bond is strongly hybridized implying that the bond is at least partially covalent. The electronic conduction can no longer be neglected. The electronic properties should be different for the two compounds. The lead-based materials should be regarded more as a semiconductor rather than an insulator, but with the specification that the electronic properties could be affected by the ferroelectric polarization.

Most models combines thermodynamics with electrostatics, majority of them deliberately neglecting the presence of free carriers and the time/frequency response of the charged defects known as traps. The perfect exponent is the "dead layer" model used to explain the thickness dependence of some dielectric/ferroelectric properties such as the dielectric constant and the coercive filed [3-7]. This model reduces the metal-ferroelectric-metal (MFM) structure to a simple, serial, connection of capacitors with fixed geometric dimensions and using constant electric fields, despite the numerous indications that the usual electrodes, like Pt, form Schottky contacts with the PZT and there is a band-bending near the electrode interface [8-13]. There are some important drawbacks of the models proposed until now to explain various experimental phenomena observed in PZT thin films:

- The investigation of the electric/ferroelectric properties were in generally performed on polycrystalline thin films, neglecting the effect of the grain boundaries and considering the films as homogenous in structure and composition.
- A model working well for a given ferroelectric material might not be suited for another material. The ferroelectric polarization is, ultimately, a microscopic property, therefore it is very sensitive to the local potentials and atom arrangements.
- The dipolar properties, represented by the ferroelectric polarization, are considered dissociated from the electronic properties, despite the fact that the polarization is, in fact, a charge that might alter the local potentials and fields, with direct impact on band structure and charge transport.

Due to these drawbacks there is a lot of inconsistency and lack of coherency in the models advanced to explain the results of the various electrical measurements usually performed on MFM structures, among which the most important are: the hysteresis loop, the capacitance-voltage characteristic (C-V), and the current-voltage characteristic (I-V). In the present paper the results obtained on epitaxial PZT thin films are explained in the frame of the same model, which considers the PZT film as a wide-gap semiconductor with Schottky contacts and electrically active traps.

2. Samples preparation and experimental methods

The studies were performed on PZT thin films having a Zr/Ti ratio of 20/80. The substrate was a single crystal $SrTiO_3$ doped with 0.5 % Nb. The growth method was the Pulse Laser Deposition (PLD). First a layer of about 80 nm thickness of $SrRuO_3$ was deposited as bottom electrode, then the PZT film was deposited from a ceramic target with a composition of $Pb_{1.1}(Zr_{0.2}Ti_{0.8})O_3$. The thickness of the PZT film was estimated to about 215 nm from Transmission Electron Microscopy (TEM) pictures. The quality of the bottom electrode and of the PZT film

was analyzed using X-ray diffraction (XRD), TEM, and Atomic Force Microscopy (AFM). The results strongly suggest that the PZT film is epitaxial, with very smooth surface, and with a low density of 90 ^{o} domains. Top $SrRuO_3$ electrodes, with an area of 0.275 mm^2, were deposited by PLD for electric measurements.

The hysteresis loop measurements were performed both in the dynamic and the static mode using a TF2000 Analyzer (AixACCT). The voltage waveform was triangular. The C-V measurements were performed using a HP 4194A Impedance/Gain Analyzer, while the I-V characteristics were obtained using a Keithley 6517 electrometer. For capacitance-frequency (C-f) and conductance-frequency (G-f) measurements at different temperatures the samples were inserted into a tubular oven with a temperature sensor placed near the PZT film.

3. Results

1. Hysteresis. The hysteresis loops obtained at different frequencies are presented in the Fig. 1a and b for both dynamic and static modes. The remnant polarization is about 40 $\mu C/cm^2$ and appears to be frequency independent. The coercive voltage, on the other side, shows a strong frequency dependence. A nice, linear, saturation domain can be observed, with a clockwise tilt of the loop with increasing the frequency of the triangular voltage. In order to extract the true ferroelectric polarization, the loops have to be corrected with the linear term, knowing that the recorded quantity is in fact the electric displacement D:

$$D = \varepsilon_0 \varepsilon_{st} E + P_S \tag{1}$$

where ε_{st} is the static dielectric constant (the linear part), E is the electric field and P_S is the true ferroelectric polarization, known also as spontaneous polarization. The ε_{st} was estimated from the linear, saturated, part of the loops. The corrected static loops are shown in the inset of Fig. 1b. Both the remnant polarization and the coercive voltage appear to be frequency independent in this case. The correction of the dynamic loops leaves unchanged the frequency dependence of the coercive voltage. The clockwise tilt of the loop also remains, while in the case of the static mode measurements the tilt is lifted after correction. These results cannot be explained only by domain walls movement, as long as in the static mode a relaxed and well saturated polarization leads to an anomaly high dielectric constant (37,000 at 1 Hz, and 3,900 at 100 Hz). This aspect will be discussed later in more detail.

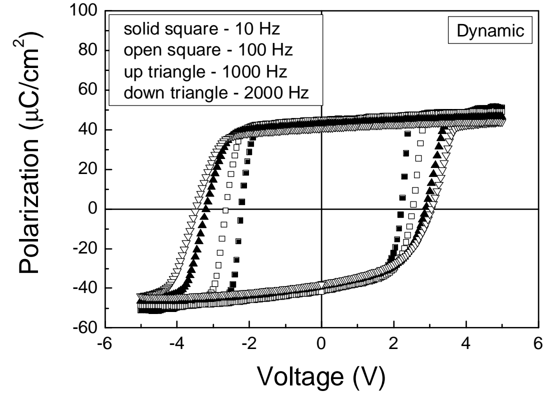

a)

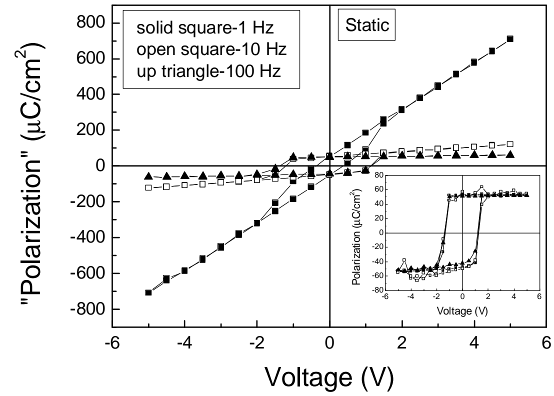

b)

Fig. 1. Hysteresis loops obtained in the dynamic mode (a) and static mode (b).

2. C-V measurements. The C-V characteristics at different frequencies are presented in the Fig. 2a. A sharp peak/discontinuity can be observed in capacitance, for both positive and negative polarities. The film was then poled by applying a –5 V voltage on the top electrode, then the C-V characteristic was raised again by sweeping the voltage up and down between 0 and +5 V. The result is shown in the Fig. 2b. It is clearly seen that the capacitance peak/discontinuity is related with the polarization reversal, being present when the voltage is swept up to +5 V (the reversal take place) and absent when the voltage is swept down to 0 V (no reversal take place). This finding suggests that the C-V characteristic and the hysteresis loop are, in fact, representations of the same phenomena: the polarization reversal.

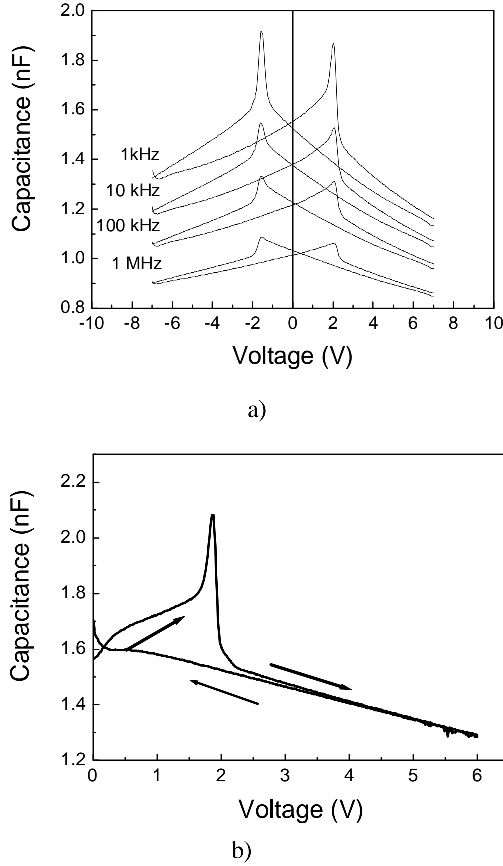

Fig. 2 C-V characteristics. Normal sweeping (a) and positive sweeping (b) after pre-poling the film in opposite direction.

An open question is the origin of the voltage dependence of the capacitance. According to Figs. 2a and b, the voltage dependence in-between the coercive voltages is due to polarization reversal. Outside the coercive voltages the capacitance can vary with the applied voltage either due to the field dependent dielectric constant, or due to a voltage dependent thickness. The first assumption is preferred in MFM models based on the simple series connection of two interface and one bulk ferroelectric capacitors with fixed geometric dimensions. The second possibility is valid for standard Schottky contacts, where the interface capacitance is voltage dependent. That leads to a voltage dependent depletion depth, therefore, the thickness of the series connected interface and bulk ferroelectric capacitors are no longer constants. In order to decide which assumption is valid is better to analyze the Fig. 3a, where the hysteresis loops are presented on the same graph with the C-V characteristic. According to the hysteresis loops in the polarization saturation domain the dielectric constant is field independent. Assuming fixed geometric dimensions, then the overall capacitance of the MFM structure should be constant outside the coercive voltages. This is not the case, the capacitance is not voltage independent outside the coercive voltages, and because the dielectric constant is voltage independent on this voltage domain it can be concluded that the voltage dependence is produced by the voltage variable depletion depth that is present near a Schottky contact. The important consequence is that the C-V characteristic can be used to extract the free carrier concentration in the same manner as in the case of a normal metal-semiconductor Schottky contact. The general formula is [14]:

$$c(T) = \frac{2}{qA^2\varepsilon_0\varepsilon_{st}\left[d\left(1/C^2\right)/dV\right]} \tag{2}$$

where c(T) is the concentration of the free carriers at the temperature T, A is the electrode area, and ε_{st} is the low frequency (static), field independent, dielectric constant. Equation (2) was deduced without making any assumption on the voltage dependence of the capacitance, therefore it can be used to extract the spatial dependence of the free carrier concentration, known also as the "doping" profile. Fig. 3b shows an example of application of equation (2) to the studied MFM structure. The free carrier concentration is about 3×10^{18} cm^{-3}, independent of the frequency of the small amplitude ac signal. It was found that this value is also temperature independent, suggesting a completely ionized shallow impurity.

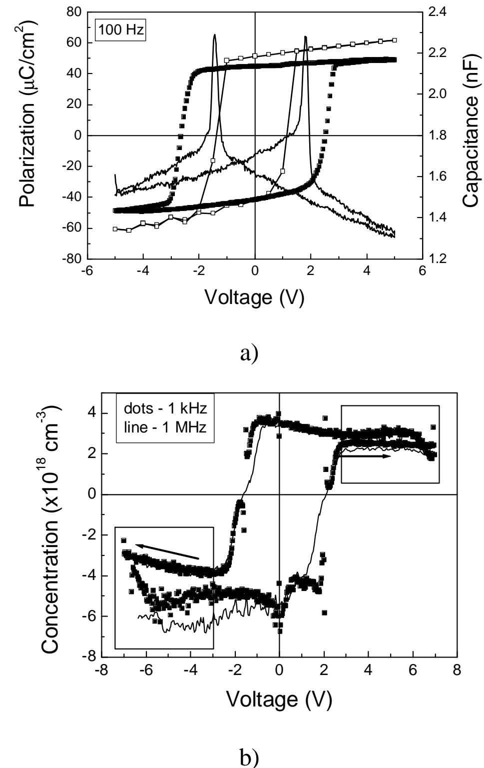

Fig. 3. (a) Hysteresis loops and C-V characteristic showing the voltage dependence of capacitance in the saturation domain of ferroelectric polarization. (b) The concentration 'hysteresis" obtained using equation (2).

3. I-V measurements. The I-V characteristics are presented in the Fig. 4. These were measured after poling the film with –5 V on the top electrode, then sweeping up the voltage from 0 to +5 V in two consecutive runs with the same delay time. As can be seen, an anomalous current peak occurs at the first run, even the delay time was as long as 10 seconds. The peak is not present at the second run, suggesting that it is related with the ferroelectric polarization reversal. The magnitude of the peak is dependent on the delay time, but the rest of the I-V characteristics is almost identical no matter the delay was 1 or 10 seconds. Some differences occur at high voltages, when the current for long delay is higher than the current for short delay time. That it is probably due to the beginning of the time dependent breakdown of the MFM structure.

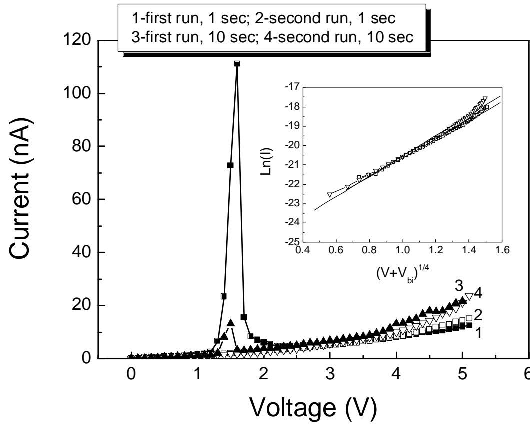

Fig. 4. I-V characteristics.

The most probable conduction mechanism is the Schottky emission [15-17]. To be coherent with the interpretation of the C-V results, the electric field used in the current density equation must be the maximum field at the Schottky contact, and not a constant field over the film thickness. The correct Schottky representation is in this case [18]:

$$\ln(J) \sim \frac{q}{kT}\sqrt[4]{\frac{q^3 N_{eff}}{8\pi^2 \varepsilon_0^3 \varepsilon_{op}^2 \varepsilon_{st}}}(V + V_{bi}^{'})^{1/4} \quad (3)$$

It means that N_{eff} can be estimated from (3) if the two dielectric constants are known from other independent measurements. The Schottky representation is shown in the inset of Fig. 4 for the true leakage currents (second runs). A value of about 1.8×10^{19} cm^{-3} was obtained for N_{eff}. This is one order of magnitude higher than the density of the free carriers deduced from the C-V measurements. Considering that N_{eff} is a fixed charge density, it means that the concentration of deep, charged, traps in the depletion region is large, exceeding the concentration of shallow impurities. The deep traps can have a serious influence on electrical measurements. The emission time τ constant is the important quantity [14]:

$$\tau_{n,p} = \left[\sigma_{n,p} v_{th,n,p} N_{C,V} \exp\left(-\frac{E_A}{kT}\right)\right]^{-1} \quad (4)$$

σ is the capture cross-section, v_{th} is the thermal velocity, $N_{C,V}$ is the density of states in the conduction or valance band, E_A is the activation energy of the trap, and k is the Boltzmann's constant. The index n and p refers to electrons and holes, respectively. The emission time constant controls the emission current from the traps [14]:

$$I_{tr}(V) = \frac{qAw_t N_{T0}}{\tau}\exp\left(-\frac{t}{\tau}\right) = \frac{qAw_t N_{T0}}{\tau}\exp\left(-\frac{V}{4\tau V_a f}\right) \quad (5)$$

w_t is the depletion width, or can be the thickness occupied by the traps if these are distributed non-uniformly near the interface. N_{T0} is the density of the occupied traps at the beginning of the measurement. For long measuring times the emission current from the traps is negligible because the term $\exp(-t/\tau)$ tends to zero. For $t<\tau$ or high frequencies the exponential term in (5) approaches unity and the emission time current becomes constant. This current component is important in the case of hysteresis measurements, which are based on an integrated charge. The integrated charge in the case of a triangular voltage, neglecting the leakage current, and at frequencies were the trap emission current is constant, is given by:

$$Q_s(V) = \left(C_l + \frac{qAw_t N_{T0}}{4\tau V_a f}\right)V + P_S(V) \quad (6)$$

As can be seen, the trapped charge behaves like a parallel connected capacitance, leading to high values of the dielectric constant. Its contribution decreases with increasing of the frequency.

The presence of deep traps was tested by performing some capacitance-frequency (C-f) and conductance-frequency (G-f) measurements at different temperatures. The recorded spectra are presented in the Fig. 5. A low frequency relaxation can be observed in the C-f characteristic, accompanied by a maximum in the G/ω - f spectra. These are signs that at least a trap level is emptying in the given temperature range (up to 300 °C). Returning to the I-V measurements, it can be assumed that the integral of the current peak will give something proportional with the ferroelectric polarization. The surface charge density obtained in this way is about 60 μC/cm² at RT and 4000 μC/cm² at 170 °C. The last values are far too high for the ferroelectric polarization. The only conclusion is that this current peak might be triggered by the polarization reversal, but it is mainly due to the current emission from the traps located in the interface region. The reversal process itself is rapid and cannot explain the presence of a current peak at delay times of 10 seconds. The compensation of the polarization charge after reversal

can be a longer process if it is performed with trapped charges. This can explain the presence of the current peaks in the I-V characteristic at such long delay times.

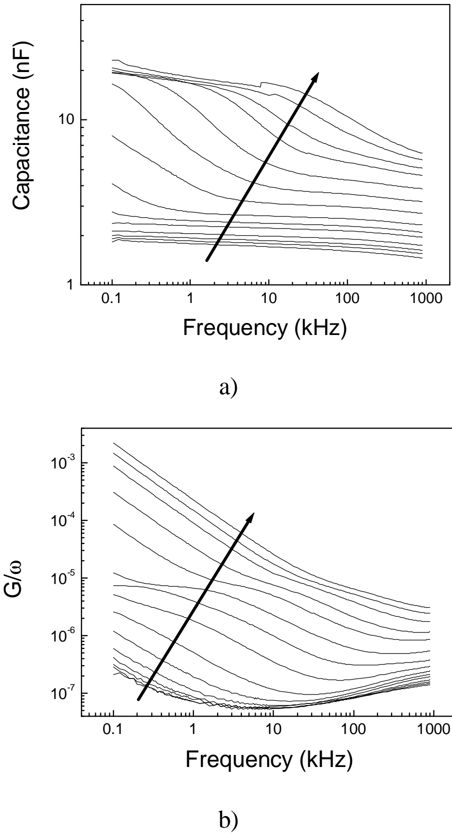

Fig. 5. C-f dependence (a) and G/ω-f dependence (b) for various temperatures.

4. Model and discussion

It is clear that the above experimental results cannot be explained in the frame of the rigid, insulator - dielectric model, which considers only the mechanical movement of the domain walls and neglects any interaction of the polarization charge with other charges that might be present in the material. In an ideal material the polarization is present under the form of two sheets of surface charges of opposite signs. It can be assumed that in this case no other polarization charge is present except these two sheets of surface charges located at a finite distance from the physical electrode-ferroelectric interface. The polarization charges must interact with other charges that are present in the system. This interaction must have influence over the local band structure, as the band-bending near the electrode interfaces, and over the charge transport through the MFM structure. The band diagram of the MFM structure is presented in the Fig. 6. The diagram was sketched assuming a p-type material with Schottky contacts and with a deep acceptor type level. Details about the model and calculation of the apparent built-in potential can be found elsewhere [15]. This is given by:

$$V_{bi}' = V_{bi} \pm \frac{P}{\varepsilon_0 \varepsilon_{st}} \delta \tag{7}$$

All the other specific quantities for a Schottky contact are dependent on the built-in potential, therefore will be affected by the ferroelectric polarization. A sudden change in the polarization orientation (reversal) means a change of the signs of the two sheets of charges located near the interfaces. This triggers a sudden change of the apparent built-in potential given by (7). A first consequence of this change is the capacitance peak/discontinuity observed in the C-V characteristic. A sudden change in the band-bending means that trapping levels that initially were below the Fermi level, goes above the Fermi level at one interface, while at the other interface the reverse phenomena take place. In the absence of polarization this phenomena is reversible, thus the traps will fill and empty no matter the voltage is swept up or down. With polarization this process is irreversible. Once the polarization is saturated in one direction, the band-bending will remain the same no matter the voltage is swept up or down without reversal. That leads to the butterfly shape of the C-V characteristic.

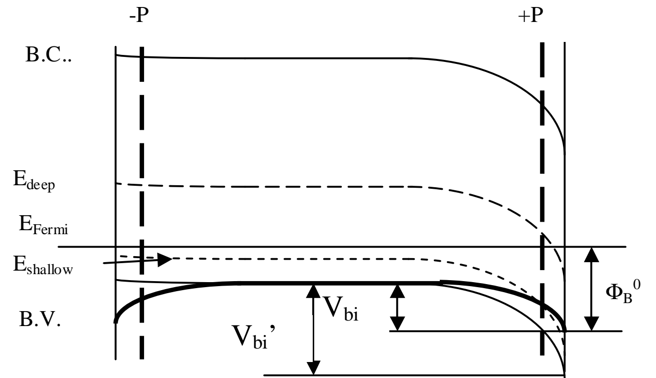

Fig. 6. The band-diagram of the MFM structure with Schottky contacts and polarization sheets of charge of opposite sign.

The same band-bending occurs also in the case of the hysteresis measurement. It means that the emission current from the traps adds to the leakage and displacement currents, making its contribution to the integrated charge and the shape of the loop especially at frequencies below the 1/τ, with τ the emission time constant of the trap.

The present model can explain also the thickness dependence of the dielectric constant. It can be adapted to explain the imprint, by a not uniform distribution of the trapped charges, and probably can be developed to explain also the fatigue phenomena [19,20]. It has to be noted that fatigue was observed only in the case of the metal electrodes like Pt. The present structure is with conductive oxide electrodes, thus the fatigue was proved to be absent. Assuming that the oxygen vacancy accumulation at the electrodes is the right model for fatigue, then it results that in the case of conductive oxides this phenomena is not present, probably because the oxide support acts as sink

for the oxygen vacancies. Therefore, the traps involved in the present study in the compensation of the polarization charge might not be the same with the traps involved in fatigue.

5. Conclusions

The present study shows that the results of the most popular electric measurements performed on MFM structure, together with some other interesting phenomena such as thickness dependence of the dielectric constant or imprint can be coherently explained in the frame of the same simple model. The model consider the ferroelectric PZT as a p-type, wide gap semiconductor, and applies the standard formalism for a metal-semiconductor Schottky contact to the MFM structure. The breakthrough is that the model directly link the polarization charge with the electronic properties, more precisely the band-bending near the electrode interfaces, and takes into consideration the time/frequency response of the deep traps. The last process has serious implications on the hysteresis measurement, which is a purely ac process, on the C-V, C-f, and G-f measurements, which are combinations of ac and dc processes, but also on the I-V measurement, which is a dc process.

Further studies are needed in order to elucidate the nature of the traps and to find the elements controlling the potential barriers at the interfaces.

Acknowledgements

Part of this work was supported by Volkswagen Stiftung within the project 'Nano-sized Ferroelectric Hybrids' under contract No. I/77737 and I/80897 and part by the CERES project *POLTRANSF.*

References

[1] M. E. Lines, A. M. Glass, Oxford, Clarendon Press, 1977.
[2] Ronald E. Cohen, Origin of ferroelectricity in Perovskite oxides, Nature **358**, 136 (1992).
[3] S. L. Miller, R. D. Nasby, J. R. Schwank, M. S. Rodrigues, P. V. Dressendorfer, J. Appl. Phys. **68**, 6463 (1990).
[4] N. A. Pertsev, J. Rodrigues Contreras, V. G. Kukhar, B. Hermans, H. Kohlstedt, R. Waser, Appl. Phys. Lett. **83**, 3356 (2003).
[5] C. Basceri, S. K. Streiffer, A. I. Kingon, R. Waser, J. Appl. Phys. **82,** 2497 (1997).
[6] B. Chen, H. Yang, J. Miao, L. Zhao, L. X. Cao, B. Xu, X. G. Qiu, B. R. Zhao, J. Appl. Phys. **97**, 024106-1 (2005).
[7] M. Grossman, O. Lohse, D. Bolten, U. Boettger, T. Schneller, R. Waser, Appl. Phys. Lett. **80**, 1427 (2002).
[8] J. F. Scott: Ferroelectric Memories, Berlin, Springer Verlag, 2000.
[9] S. Dey, P. Alluri, J. J. Lee, Integrated Ferroelectrics. **7**, 341 (1995).
[10] Y. S. Yang, S. J. Lee, S. H. Kim, B. G. Chae, M. S. Jang, J. Appl. Phys. **84**, 5005 (1998).
[11] J. Lee, C. H. Choi, B. H. Park, T. W. Noh, J. K. Lee, Appl. Phys. Lett. **72**, 3380 (1998).
[12] B. H. Park, S. J. Hyun, C. R. Moon, B. D. Choe, J. Lee, C. Y. Kim, W. Jo, T. W. Noh, J. Appl. Phys. **84**, 4428 (1998).
[13] S. Sadashivan, S. Aggarwal, T. K. Song, R. Ramesh, J. T. Evans Jr., B. A. Tuttle, W. L. Warren, D. Dimos, J. Appl. Phys. **83,** 2165 (1998).
[14] D. K. Schroeder: Semiconductor material and device characterization. New York, Wiley-Interscience, 1998.
[15] L. Pintilie, M. Alexe, J. Appl. Phys. in press.
[16] L. Pintilie, I. Boerasu, M. J. M. Gomes, T. Zhao, R. Ramesh, M. Alexe, J. Appl. Phys. in press.
[17] C. Shudhama, A. C. Campbell, P. D. Maniar, R. E. Jones, R. Moazzami, C. J. Mogab, J. C. Lee, J. Appl. Phys. **75**, 1014 (1994).
[18] I. Boerasu, L. Pintilie, M. Pereira, M. I. Vasilevskyi, M. J. M. Gomes, J. Appl. Phys. **93**, 4776 (2003).
[19] G. LeRhun, G. Poullain, R. Bouregba, J. Appl. Phys. **96**, 3876 (2004).
[20] J. F. Scott, M. Dawber, Appl. Phys. Lett. **76,** 3801 (2000).

Invited Lecture

*Corresponding author: pintilie@infim.ro